STRUCTURE/PROPERTY RELATIONSHIPS IN

SOLID-SOLUTION STRENGTHENED SUPERALLOYS

D. L. Klarstrom, H. M. Tawancy, M. F. Rothman Cabot Corporation, Kokomo, Indiana 46901, USA

Summary

Fabrication procedures can alter the microstructure and, hence, the properties of solid-solution strengthened superalloys. The extent of such changes was investigated through experiments designed to simulate component manufacture. Experiments were also conducted to examine the effects of simulated in-service conditions on the microstructures, mechanical properties and weldability of these alloys.

Introduction

Solid-solution strengthened superalloys are among the most widely used materials for demanding, long-time applications at elevated temperatures. They experience such general acceptance because of their unique combination of high temperature strength, resistance to aggressive high temperature environments, and superior fabricability. The properties of these materials have generally been determined for the solution heat treated condition in which they are normally supplied. In this condition, the alloys display an optimum combination of properties for room temperature fabrication and elevated temperature service. Component manufacturing operations, however, can significantly alter the microstructure and, therefore, the properties of the originally supplied material. It was the purpose of this study to investigate the extent of such changes through experiments involving thermal and mechanical cycles to simulate component manufacturing. The microstructural changes produced by such treatments were studied in detail, and the resultant creep properties at a selected condition were determined.

Another important aspect in the use of solid-solution strengthened superalloys concerns response to in-service conditions in terms of structure/property effects. To examine this, samples were exposed at temperatures in the range of 650°-980°C (1200°-1800°F), and the resultant microstructural changes were documented. The residual room temperature tensile properties and the weldability of the exposed materials were also determined to assess property degradation generally, as well as to address the practical subject of weld repairability.

Materials and Procedures

The nominal compositions of the alloys studied in this investigation are shown in Table I. These materials were commercially produced, cold rolled sheet 1.0-1.3~mm (0.040-0.050~in.) thick. Sheet in alloys X, 188 and 230 were produced by Cabot Corporation, alloy 617

Table I

Nominal Compositions of Alloys

Alloy	Ni	Co	Cr	Мо	W	Fe	_Si_	Mn	c_	<u>A1</u>	Others
HASTELLOY® alloy X	BAL	1.5	22	9	0.6	18.5	1.0*	1.0*	0.10		
HAYNES [®] alloy No. 188	22	BAL	22		14	3.0*	0.35	1.25*	0.10		0.04 La
HAYNES [®] Developmental alloy No. 230	BAL	3.0*	22	2	14	3.0*	0.40	0.50	0.10	0.30	0.03 La
INCONEL® alloy 617	BAL	12.5	22	9		1.5	0.50	0.50	0.07	1.20	0.3 Ti
NIMONIC alloy 86	BAL		25	10		5.0*	1.00*	1.00*	0.05		.015 Mg, 0.03 Ce

^{*} Maximum

^{*} HASTELLOY and HAYNES are registered trademarks of Cabot Corporation INCONEL and NIMONIC are registered trademarks of Inco Family of Companies

sheet was produced by Huntington Alloys, Inc., and alloy 86 sheet was produced by Wiggin Alloys, Ltd. All materials were received in the solution heat treated condition. Recommended solution heat treatment temperatures are 1150°C (2100°F) for alloy 86, 1175°C (2150°F) for alloys X, 188 and 617, and 1230°C (2250°F) for alloy 230. A summary of the as-received tensile properties is given in Table II.

Table II
Summary of As-Received Properties

		RT Tensile Properties					ties
		0.2%	Y.S.		U'	TS	% EL
<u>Alloy</u>	ASTM G.S.	MPa	(ksi)		MPa	(ksi)	in 50 mm (2 in.)
X	5-6	380	(55)		765	(111)	44
188	5.5-6	480	(70)		950	(138)	53
230	5-6	385	(56)		870	(126)	48
617	3-4	335	(49)		740	(107)	60
86	3.5-6	370	(54)		785	(114)	55

To simulate strain encountered in fabrication operations, sheet samples measuring approximately 205 mm x 510 mm (8 inches x 20 inches) were stretched using a stretcher leveling device. Test specimen blanks were subsequently sheared from the strained sheet and heat treated in an air atmosphere furnace. No attempt was made to remove the oxidized surface layer developed on the samples during heat treatment prior to testing.

In-service effects were simulated by exposing unstressed samples in an air atmosphere furnace for a period of 1000 hours at selected temperatures in the range of 650°-980°C (1200°-1800°F). Room temperature tensile tests were performed on the samples in the as-exposed condition. The weldability of the exposed samples was investigated using the spot varestraint TIG-A-MA-JIG test (1). Prior to this testing, the sample surfaces were vapor blasted using a suspension of alumina in water.

Results and Discussion

Fabrication Simulation

The fabrication of components from superalloy sheet materials involves

thermomechanical and thermal treatments such as forming and annealing, stress relieving, and brazing. These operations add to the thermomechanical history of the material, and, therefore, differences between the original and final properties can be expected to occur. Furthermore, it may not be feasible for the fabricator to adhere to the recommended heat treatment practices due to the need to avoid or minimize part distortion, due to equipment limitations, or due to the inability to match brazing and solution heat treatment conditions.

To assess the effects of thermomechanical cycles in which the heat treatment was performed at a temperature below the recommended solution heat treatment temperature, samples were strained 10 percent and annealed at temperatures of 1040°C (1900°F) and 1120°C (2050°F). The effects of these treatments on the creep properties at 870°C (1600°F)/48 MPa (7 ksi) are presented in Table III. It can be seen that the cycle involving an anneal at 1040°C (1900°F) resulted in significantly higher creep lives in all cases. The cycle employing an anneal at 1120°C (2050°F) resulted in a general reduction in creep life except for alloy 188 which was significantly stronger. Microstructural analysis of the 1040°C (1900°F) annealed samples revealed in all cases the presence of residual strain as evidenced by slightly bent twins and carbide decorated slip bands. Heavy carbide precipitation was also noted at twin and grain boundaries as illustrated in Figure 1. Samples given the 1120°C (2050°F) anneal exhibited varied microstructures. Alloys X and 86 were found to have undergone complete recrystallization to grain sizes similar to those in the as-received condition. Their microstructures also contained a remnant carbide delineation of the original grain boundaries as shown in Figure 2. Alloys 188, 230 and 617 remained essentially unrecrystallized with grain boundary and

Table III

Effects of Thermomechanical Cycles On
870°C (1600°F)/48 MPa (7 ksi) Creep Properties

Time To Indicated Creep Strain, Hrs.

Alloy	As-Rec 0.5%	eived 1.0%	1040° 0.5%	10% Strain + 1 C (1900°F) 1.0%	Heat Treatme 1120°C 0.5%	nt* (2050°F) 1.0%
x	13	26	93	182	5	12
188	162	334	549	> 1000**	680	> 900**
230	88	221	1035	> 1510**	50	150
617	66	160	840	> 1510**	49	200
86	18	26	310	595	5	13

^{* 5-15} Min. at Temperature/Air Cool

^{**} Test Discontinued

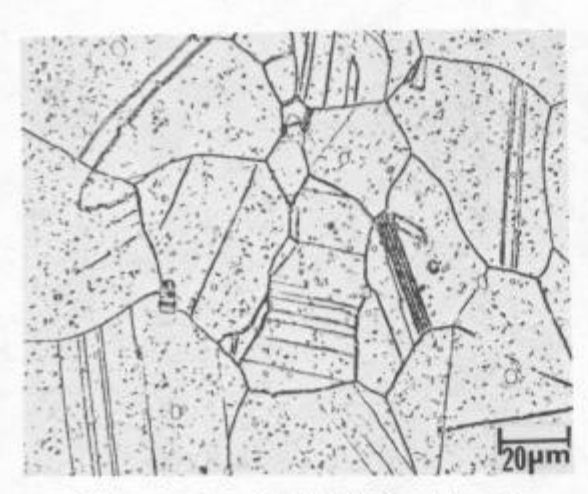


Figure 1: HASTELLOY alloy X sheet cold-worked 10% and annealed at 1040°C (1900°F)/15 minutes/AC.

intragranular carbide precipitation much in evidence, but the carbides were noted to be coarser and not as abundant as in the case of the 1040°C (1900°F) anneal. Some areas in the microstructures of alloys 188 and 230 were also noted which showed signs of partial recrystallization as illustrated in Figure 3.

To investigate the effects of thermal treatments in the absence of mechanical strain (e.g., brazing cycles), samples were subjected to anneals at temperatures of 1040°C (1900°F), 1120°C (2050°F) and 1175°C (2150°F) for 5-15 minutes and air cooled. The resultant 870°C (1600°F)/48 MPa (7 ksi) creep

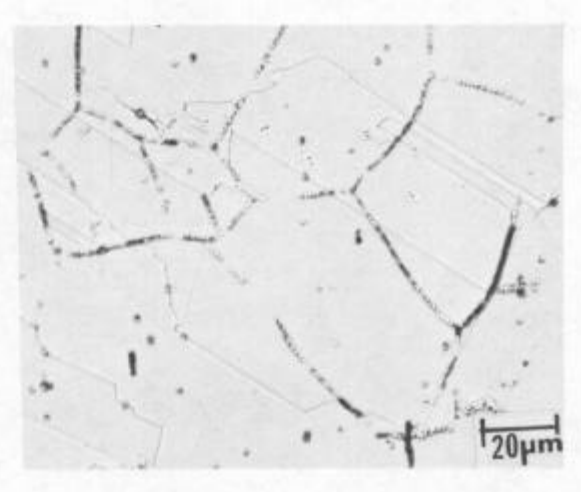


Figure 2: NIMONIC alloy 86 sheet cold-worked 10% and annealed at 1120°C (2050°F)/15 minutes/AC.

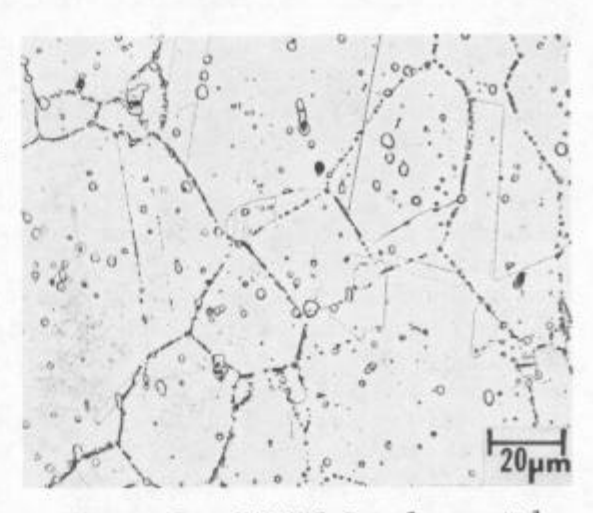


Figure 3: HAYNES Developmental alloy No. 230 sheet cold-worked 10% and annealed at 1120°C (2050°F)/15 minutes/AC.

properties obtained are summarized in Table IV. Generally, the thermal treatments caused a degradation in the as-received creep properties, the magnitude of which was temperature and alloy dependent.

For alloys X and 188, both of which precipitate secondary M_6C -type carbides, a similar response pattern is evident. Both displayed an insensitivity to annealing temperature, the residual creep strength level being essentially the same for all three conditions, allowing for the normal scatter associated with creep test data. Alloys 230 and 617, which both precipitate $M_{23}C_6$ -type secondary carbides, also displayed a similar response pattern. Both exhibited a large creep life reduction with the $1120\,^{\circ}C$ ($2050\,^{\circ}F$) anneal, and about the same level of reduction for the $1040\,^{\circ}C$ ($1900\,^{\circ}F$) and $1175\,^{\circ}C$ ($2150\,^{\circ}F$) anneals. Alloy 86, which also precipitates $M_{23}C_6$ -type secondary carbides, behaved differently. A large creep life reduction was produced by the $1040\,^{\circ}C$ ($1900\,^{\circ}F$) anneal, while anneals at

Table IV

Effects of Secondary Heat Treatments
On 870°C (1600°F)/48 MPa (7 ksi) Creep Properties

Time to Indicated Creep Strain, Hrs. Secondary Heat Treatment* 1040°C (1900°F) 1175°C (2150°F) Alloy As-Received 1120°C (2050°F) 0.5% 1.0% 0.5% 1.0% 0.5% 0.5% 1.0% 1.0% Х 13 26 7 16 6 14 7 24 188 162 334 68 200 72 272 97 260 230 88 221 23 52 9 20 20 44 617 160 66 28 71 8 35 15 63

26

3

86

18

 1120° C (2050°F) and 1175° C (2150°F) resulted in creep lives similar to those of the as-received condition.

13

25

10

28

q

Most of the observed creep life degradation for the re-annealing treatments can be explained on the basis of carbide precipitation phenomena. Temperatures of $1040\,^{\circ}\text{C}$ ($1900\,^{\circ}\text{F}$) and $1120\,^{\circ}\text{C}$ ($2050\,^{\circ}\text{F}$) are below the secondary carbide solvus temperatures for most of the alloys. Exposure of the alloys to these temperatures caused secondary carbide precipitation which depleted the originally supersaturated matrices of carbon. In this condition, less carbide precipitation on dislocations occurs during creep, and lower creep lives result. Alloy 86 annealed at $1120\,^{\circ}\text{C}$ ($2050\,^{\circ}\text{F}$) appears to be an exception to this explanation. However, it is likely that $1120\,^{\circ}\text{C}$ ($2050\,^{\circ}\text{F}$) is at or above the $120\,^{\circ}\text{C}$ solvus temperature for the alloy.

In several of the foregoing cases, 1175°C (2150°F) represented the solution heat treatment temperature, but a degradation of creep strength was noted. Such behavior strongly suggested that cooling practice from the annealing temperature might be a controlling parameter. To examine this possibility, samples of alloys X, 188 and 617 were solution annealed at 1175°C (2150°F) and cooled at various rates ranging from a water quench to a furnace cool between 1175°C (2150°F) and 650°C (1200°F). The effects of these treatments on $870^{\circ}\text{C} (1600^{\circ}\text{F})/48 \text{ MPa} (7 \text{ ksi}) \text{ creep properties are given in Table V.}$ Surprisingly, alloy X displayed the same creep strength regardless of the manner in which it was cooled. Alloy 188 exhibited creep properties equivalent to the original material in the water quenched condition, but a degradation in strength occurred as the cooling rate decreased. Alloy 617 displayed a marked creep life improvement in the water quenched condition, but a significant degradation resulted with the slower cooling rates. For alloys 188 and 617, matrix carbon depletion by carbide precipitation during the slower cooling cycles provides a satisfactory explanation of the observed behavior. Carbon supersaturation is also the likely cause for the increased creep strength of alloy 617 in the water quenched condition.

^{* 5-15} minutes at Temperature/Air Cool

Temperature On 870°C (1600°F)/48 MPa (7 ksi)
Creep Properties

Time	to	Indicated	Creep	Strain,	Hrs.
------	----	-----------	-------	---------	------

				Solution Heat Treated at 11/5°C (2150°F)/5 min.						
				and Cooled as Indicated*						
	As-Red	ceived	W	IQ	AC	;	FC to 650°C	(1200°F)/A	'C	
<u>Alloy</u>	0.5%	1.0%	0.5%	1.0%	0.5%	1.0%	0.5%	1.0%		
X	13	26	8	15	7	24	6	13		
188	162	334	148	405	97	260	48	110		
617	66	160	302	540	15	63	9	19		

^{*} WQ = Water Quench AC = Air Cool FC = Furnace Cool

insensitivity to cooling rate displayed by alloy X, on the other hand, is somewhat puzzling. Since the creep properties were the same regardless of cooling method, it is believed that the residual matrix carbon level was the same in all cases. This could have occurred not only through carbide precipitation during cooling, but also by carbide precipitation occurring at the creep test temperature both before and after the sample was loaded.

In-Service Simulation

Prolonged in-service exposure of solid-solution strengthened superalloys generally results in a reduction of room temperature ductility because of the precipitation of secondary carbides and/or topologically closed-packed phases. To examine for this, samples were exposed at selected temperatures in the typical use temperature range of 650°-980°C (1200°-1800°F). The resultant room temperature tensile elongations obtained are summarized in Table VI. Typical optical micrographs for alloys X and 230 for all exposure conditions are shown in Figures 4 and 5, and for alloys 188, 617 and 86 for the 760°C (1400°F) exposure condition in Figure 6.

For alloy X, the ductility reductions following exposures at 650°C (1200°F) and 760°C (1400°F) can be attributed to $\rm M_{23}C_6$ and sigma-phase precipitation, and the reduction following the 870°C (1600°F) exposure to $\rm M_{23}C_6$, $\rm M_{12}C$ and mu-phase precipitation (2). The small ductility decline for the 980°C (1800°F) exposure is

Table VI

Effects Of Thermal Exposures On
Room Temperature Ductility

	Room Temperature Tensile Elongation, %									
	Following 1000 Hour Exposure at Indicated Temperature									
Alloy	As-Received	650°C (1200°F)	760°C (1400°F)	870°C (1600°F)	980°C (1800°F)					
X	44	28	11	24	38					
188	53	39	15	20	41					
230	48	39	35	37	40					
617	60	39	42	29	30					
86	55	47	45	44	47					

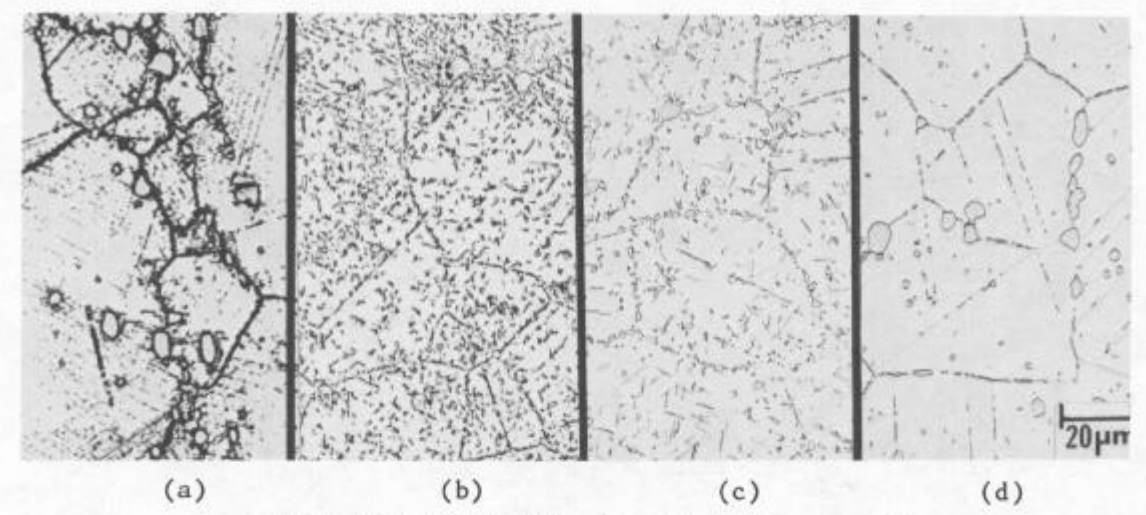


Figure 4: HASTELLOY alloy X sheet exposed for 1000 hours at various temperatures.

(a) 650°C (1200°F); (b) 760°C (1400°F);

(c) 870°C (1600°F); (d) 980°C (1800°F).

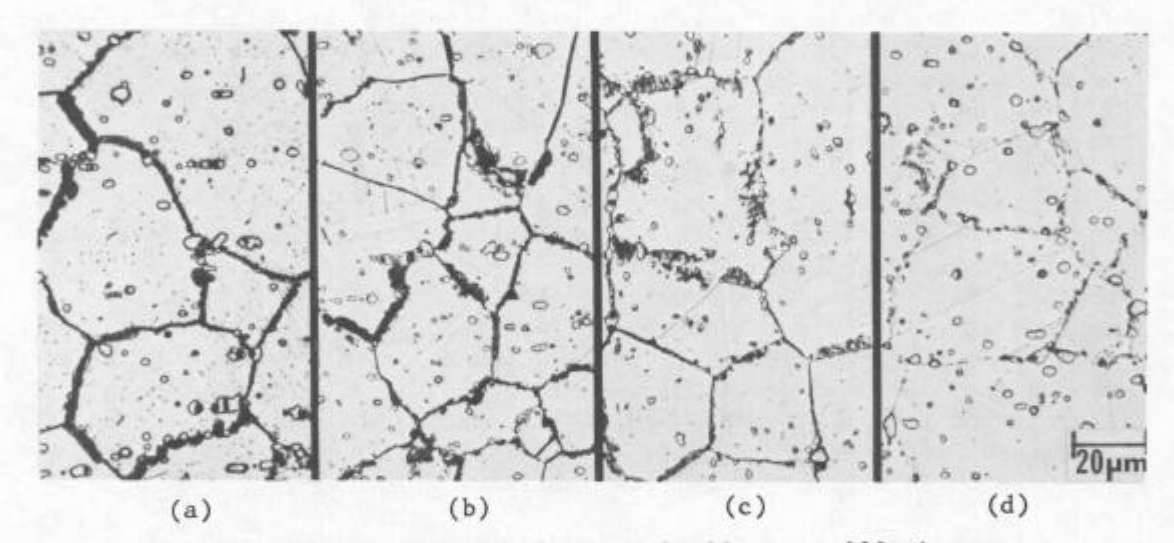


Figure 5: HAYNES Developmental alloy No. 230 sheet exposed for 1000 hours at various temperatures.

(a) 650°C (1200°F); (b) 760°C (1400°F);

(c) 870°C (1600°F); (d) 980°C (1800°F).

due to secondary M₆C precipitation. The reductions which occur in alloy 188 at 650°C (1200°F) and 980°C (1800°F) are due to M₆C precipitation, while the larger reductions resulting from exposures at 760°C (1400°F) and 870°C (1600°F) are due to M₆C, M₂₃C₆ and Co₂W-type Laves-phase precipitation (3).

Alloys 230, 617 and 86 are generic materials in the sense that $M_{23}C_6$ carbides are the only secondary phases that precipitate. This simple behavior affords the opportunity to appreciate the significance of TCP phase formation in reducing ductility as can be noted in Table VI for alloys X and 188. The lower ductility values

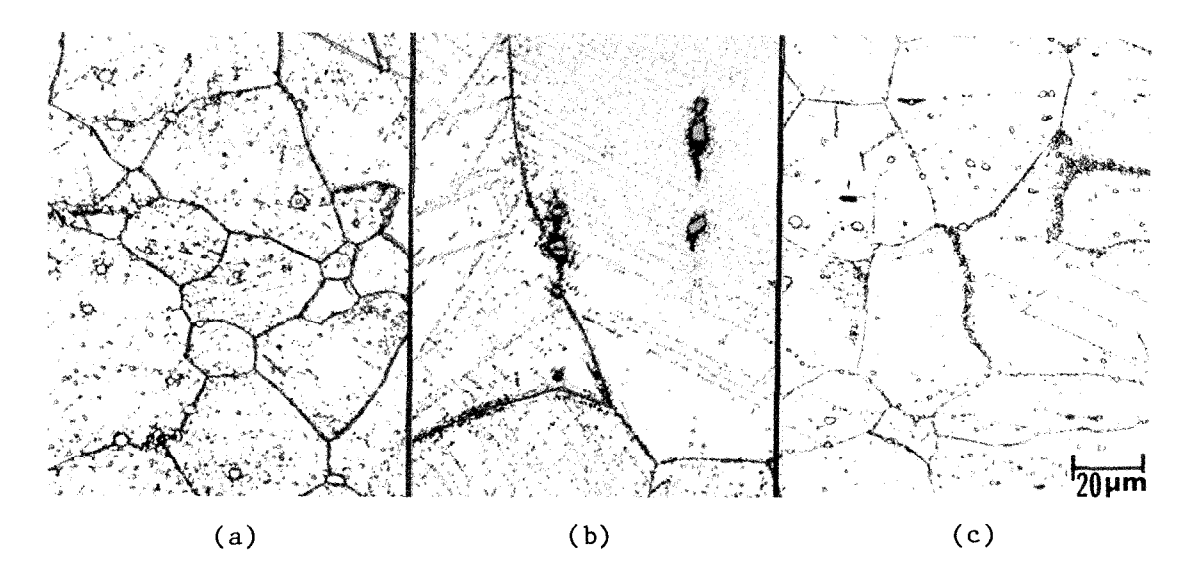


Figure 6: Microstructures for three alloys exposed for 1000 hours at 760°C (1400°F).
(a) HAYNES alloy No. 188; (b) INCONEL alloy 617; (c) NIMONIC alloy 86

observed for alloy 617 for exposures at 870°C (1600°F) and 980°C (1800°F) are not due to TCP phase precipitation, and environmentally induced damage is, therefore, suspected. At exposure temperatures of $650^{\circ}-870^{\circ}$ C (1200°-1600°F), the M₂₃C₆ precipitation occurring in these alloys typically displays a discontinuous reaction morphology which can be readily noted in the figures. In spite of this tendency, residual ductility values remain relatively high. At an exposure temperature of 980°C (1800°F), the M₂₃C₆ carbides take on a discrete, globular morphology as illustrated in Figure 5.

To gain some appreciation of the weldability of solid-solution strengthened superalloys following service, samples exposed for 1000 hours at temperatures in the 650°-980°C (1200°-1800°F) range were examined for strain induced heat-affected-zone (HAZ) cracking sensitivity using the spot varestraint TIG-A-MA-JIG test. A summary of the results obtained is presented in Table VII. It can be seen that in

Crack Initiation

Augmented Strain Required To Initiate HAZ Cracking,* %								
		Following		At Indicated Tem				
Alloy	As-Received	650°C (1200°F)	760°C (1400°F)	870°C (1600°F)	980°C (1800°F)			
X	0.62	0.52	0.60	1.01	0.69			
188	0.48	0.55	0.58	> 1.20	0.76			
230	0.48	0.52	0.46	0.79	0.76			
617	0.43	0.31	0.21	1.00	0.49			
86	0.71	0.67	0.54	> 1.40	1.00			

^{*} Average Total Crack Length > 0.25 mm (.010 inches)

most cases the exposures did not result in a degradation in HAZ cracking susceptibility. In fact, exposures at 870°C (1600°F) resulted in significant improvements for all alloys. The only cases of degradation occurred for alloy 617 exposed at temperatures of 650°C (1200°F) and 760°C (1400°F). The cause of this behavior is not known. However, the strengthening which occurs in the alloy on exposure to those temperatures (4) may be a factor.

Conclusions

It has been shown that the thermal and thermomechanical cycles which solid-solution-strengthened superalloys may experience in component fabrication or in service can induce changes in the microstructures of these materials. These structural changes can be accompanied by significant changes in mechanical properties. The sensitivity of the various alloys examined in this study to structure/property changes as a consequence of fabrication or service exposure varies with alloy, although similarities in behavior among alloys of the same "family" were noted. It is concluded that these changes in the structure and properties are an important factor for consideration by design engineers and others involved in the use of these materials.

References

- 1. C. D. Lundin et. al., "The Varestraint Test," Welding Research Council Bulletin 280, August, 1982, pp 16-18.
- 2. H. M. Tawancy, "Long-Term Aging Characteristics of Hastelloy alloy X," J. Mater. Sci., <u>18</u> (1983), pp 2976-2986.
- 3. R. B. Herchenroeder, et. al., "Haynes alloy No. 188," Cobalt, No. 54, March, 1972, pp 3-13.
- 4. W. L. Mankins, J. C. Hosier and T. H. Bassford, "Microstructure and Phase Stability of Inconel alloy 617," Met. Trans., Vo. 5, Dec. 1974, pp 2579-2589.